

Nonequilibrium critical behavior of the triplet annihilation model

Ronald Dickman

Department of Physics and Astronomy, Herbert H. Lehman College, City University of New York, Bronx, New York 10468

(Received 12 March 1990)

The nature of the critical behavior in the triplet annihilation model—which exhibits a new kind of nonequilibrium phase diagram—is elucidated through scaling analysis of time-dependent Monte Carlo simulations. The results support the hypothesis that nonequilibrium critical points in single-component reaction diffusion systems are generically in the directed-percolation or Reggeon-field-theory class.

I. INTRODUCTION

Nonequilibrium phase transitions are currently under intensive study in physics and biology.^{1,2} Some examples of interest in condensed-matter physics are surface reaction models,^{3,4} which describe the poisoning of a catalyst, and the driven lattice gas, pertinent to ionic conductors.⁵ While nonequilibrium critical points are a largely unexplored domain, they exhibit many features associated with equilibrium critical phenomena: long-range correlations, a well-defined order parameter, and singularities characterized by critical exponents.

The present work is part of an effort to delineate universality classes for nonequilibrium critical behavior. This issue has been examined recently for reaction-diffusion systems, i.e., stochastic models in which particles are created autocatalytically, disappear spontaneously, and diffuse. Since there is no spontaneous *creation* of particles, the zero-particle state or vacuum is *absorbing*. It may also be possible (in the infinite-volume limit) to sustain an “active” steady state. The critical point marks the disappearance of the active state. The order parameter is the steady-state particle density, which scales asymptotically as $\bar{\rho} \propto (\lambda - \lambda_c)^\beta$, where λ_c is the critical creation rate. A simple example is Schlögl’s first model.⁶ Its lattice analog, the contact process,^{7,8} exhibits critical behavior in the directed percolation or Reggeon field-theory (RFT) class.^{9–12} Studies of a variety of related models, employing simulations,^{13–17} field-theoretic arguments,^{10,12,13,18–20} and series expansions,^{11,14,21} all support the conjecture¹³ that RFT is the generic critical behavior for systems with a scalar order parameter and a single absorbing state. This universality class is characterized by the order-parameter exponent $\beta=0.277$ (Refs. 11 and 21) in $d=1+1$ (one space and one time dimension), and $\beta=0.585$ for $d=2+1$.¹¹

The subject of this paper is the “triplet annihilation model,” which is of the sort described above, but with the new feature that diffusion inhibits annihilation.¹⁵ The model possesses a surprising phase diagram, including a critical line marking the extinction of a population that reproduces *too rapidly*. The main purpose of the present work is to present simulation results that clarify the nature of the critical behavior in this model. In the following section I define the model. Section III describes the simulation method and scaling analysis. Results are described in Sec. IV, followed by a discussion in Sec. V.

II. MODEL

The *triplet annihilation* model or “ $D3$ model,”¹⁵ is an interacting-particle system incorporating diffusion, autocatalytic creation, and cluster annihilation among particles that occupy the sites of a lattice. The configuration of the system is described by a set of occupation variables σ_i ; $\sigma_i=0$ (1) if site i is vacant (occupied); multiple occupancy is forbidden. The evolution is a Markov process, consisting of a sequence of “moves,” each involving a single elementary process at a randomly chosen site. The elementary processes are diffusion (hopping), creation, and annihilation; they occur with probabilities D , $(1-D)\lambda/(1+\lambda)$, and $(1-D)/(1+\lambda)$, respectively. The parameters λ (creation rate) and D (diffusion rate) determine the behavior of the model.²²

The diffusion process consists in choosing a site i at random, and interchanging σ_i and σ_{i+1} . For creation, a site i and a nearest neighbor $i+e$ are picked at random. If $\sigma_i=1$ and $\sigma_{i+e}=0$, then the latter value is changed to 1 (i.e., the particle at i “creates” a new particle at the neighboring site). In the annihilation process, particles at a site i and its two neighbors are removed, if and only if all three sites are occupied. The steady-state simulations

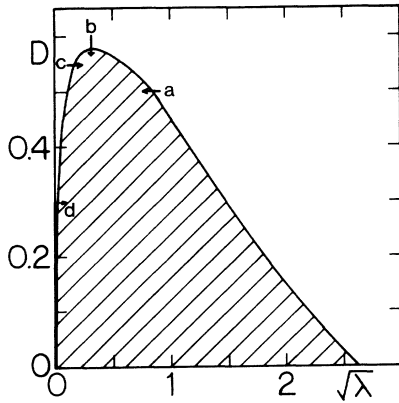


FIG. 1. Phase diagram for the triplet annihilation model. Within the shaded region, there is no active steady state. The lines indicate the range of parameter values studied in cases (a), (b), (c), and (d).

reported in Ref. 15 were performed on a one-dimensional lattice of L sites ($L = 10\,000$ or $20\,000$), with periodic boundary conditions. One time unit corresponds to L attempted moves—one per site.

The steady-state phase diagram of the triplet annihilation model is shown in Fig. 1. The main features may be summarized as follows. (Further details may be found in Ref. 15). When $D = 0$, there is a continuous transition at $\lambda_c = 6.72$, with $\beta \approx 0.28$, indicating a RFT-type critical point. This critical point shifts to smaller λ values as D is increased. (Such a shift is to be expected since, by breaking up clusters, diffusion suppresses annihilation and enhances creation.) Remarkably, there is a critical diffusion rate $D^* \approx 0.58$ above which λ_c is zero so that an active steady state is possible for any creation rate. For $0 < D < D^*$, there are in fact *two* distinct sets of creation rate values which support an active steady state: $0 < \lambda < \lambda_-$ and $\lambda > \lambda_+$; for $\lambda_- < \lambda < \lambda_+$ the only possible steady state is the vacuum. The new active steady state at very low creation rates ($0 < \lambda < \lambda_-$) results from the competition between diffusion and annihilation. A mean-field description at the pair level¹⁵ yields a prediction for the phase diagram which, while qualitatively correct, is in poor agreement with simulations. A somewhat better phase boundary has been derived via a mean-field renormalization-group calculation.²³

The simulations reported in Ref. 15 demonstrate that λ_+ is a line of RFT-type critical points, and that as $\lambda \rightarrow 0$, $\bar{\rho} \propto \lambda^{1/2}$, indicating that (for $D > 0$), $\lambda = 0$ is a mean-field-like critical line. The present work focuses on the critical behavior as $\lambda \rightarrow \lambda_-$, which could not be determined in the steady-state simulations.

III. TIME-DEPENDENT MONTE CARLO SIMULATIONS

Simulations of static nonequilibrium critical behavior are often quite difficult. In addition to the usual problems of large fluctuations, critical slowing down, and finite-size effects, simulations at the brink of an absorbing state require particular care, as one is studying a long-

lived, but intrinsically metastable state. In several cases it has been possible to gain a more precise determination of critical behavior by means of *time-dependent* simulations.^{13,16,24,25} The time-dependent approach consists in studying the evolution of the system over a large number N of independent realizations or “runs” which all begin with the same initial configuration. (In each run the (pseudo)random-number generator is initialized with a different “seed.”) Each run proceeds until some fixed maximum time t_M (unless all of the particles disappear before t_M). The lattice is sufficiently large that particles never reach the boundary before t_M . The mean values (over the set of N runs) of $n_{i,t}$ (the number of particles in run i , at time t) and related quantities are computed as functions of the parameters; their long-time behavior yields information on the critical exponents.

Following Grassberger and de la Torre,⁹ I use the initial configuration $\sigma_0 = 1$, $\sigma_i = 0$ for $i \neq 0$, and compute the following: (1) n_t , the mean of $n_{i,t}$ over the runs; (2) P_t , the survival probability (i.e., the fraction of runs with $n_{i,t} > 0$); and (3) x_t^2 , the mean-square distance of particles from the origin. x_t^2 is computed only over runs which have survived until time t , while n_t includes as well those runs which have reached the vacuum state.

The scaling hypothesis for the contact process and allied models asserts that at the critical point, the quantities defined above are governed by power laws as $t \rightarrow \infty$:

$$P_t \propto t^{-\delta}, \quad (1)$$

$$n_t \propto t^\eta, \quad (2)$$

$$x_t^2 \propto t^z. \quad (3)$$

Away from the critical point, the evolution departs from a pure power law. For example, in the subcritical regime P_t will approach an exponential decay once t exceeds some typical lifetime analogous to the longitudinal correlation length $\xi_{||}$ in directed percolation,²⁶ while in the supercritical regime P_t approaches a nonzero limit. Thus a graph of $\ln P_t$ versus $\ln t$ will show positive (negative) curvature in the supercritical (subcritical) regime. This permits one to set limits on λ_c . Similar considerations apply to n_t and x_t^2 . The asymptotic slopes of the (critical) graphs define the dynamic critical exponents δ , η , and z . In general, the asymptotic power-law behavior is modified by corrections to scaling, so that (at the critical point) P_t is more accurately represented by

$$P_t = t^{-\delta}(1 + at^{-\delta'} + \dots), \quad (4)$$

where δ' is the correction-to-scaling exponent, and the subsequent terms fall off more rapidly than $t^{-\delta'}$. (Similar expressions are expected to hold for n_t and x_t^2 .) In order to estimate the asymptotic slope, it is therefore very useful to plot the local slope

$$\delta_t = \frac{\ln(P_t/P_{t/m})}{\ln m} \quad (5)$$

against t^{-1} . (In the present study $m = 5$.) In such a plot the asymptotic slope δ can be read from the y intercept. The exponents derived from this analysis are to be com-

pared with the known $d=1+1$ directed percolation or RFT values.^{9,11}

$$\begin{aligned} \delta &= 0.162(4), \\ \eta &= 0.317(2), \\ z &= 1.272(7). \end{aligned} \quad (6)$$

(The numbers in parentheses indicate the uncertainty in the last figure.)

The preceding discussion demonstrates the need to determine quantities such as P_t and n_t , starting from a single-particle initial configuration. While it is straightforward to implement the Markov process described in Sec. II directly, the resulting simulation algorithm is very inefficient when the density is low. (Most attempted moves yield no change since a randomly chosen site is almost always vacant.) The efficiency of the simulation can be improved by choosing site i —the location for the attempted move—from a list of *occupied* sites, provided one modifies the diffusion rate and the time increment accordingly. The creation and annihilation moves are as before (but with σ_i surely equal to 1), but a diffusion move now consists in choosing an occupied site i and a nearest neighbor $i+e$ at random, and moving the particle from i to $i+e$, if $\sigma_{i+e}=0$. Let D' be the fraction of attempted diffusion moves in the new algorithm. The rates for attempted diffusive and nondiffusive moves, for a given particle, are in the ratio $D'/(1-D')$, whereas in the original formulation this ratio is $2D/(1-D)$. (The factor of 2 appears because a particle at i has *two* opportunities to diffuse—when either i or $i-1$ is chosen—in the original algorithm.) Equating these ratios yields $D'=2D/(1+D)$. In the new algorithm, creation and annihilation moves occur with probabilities $(1-D')\lambda/(1+\lambda)$ and $(1-D')/(1+\lambda)$, respectively. The time increment per move in the new algorithm is $1/n$, where n is the number of occupied sites just before the move: each attempted move now represents, on average, L/n attempts in the original algorithm. The choice of algorithm is purely a matter of computational efficiency and in no way affects the average steady-state or time-dependent properties of the model. The symbols “ D ” and “ t ” retain their original significance, given in Sec. II.

IV. SIMULATION RESULTS

The simulation method described above was used to study the dynamics of the triplet annihilation model along four trajectories in the λ - D plane.

(a) $D=0.5$, with λ varying between 0.725 and 0.717, crossing the critical line λ_+ .

(b) $\lambda=0.1$, with D varying between 0.6 and 0.58, crossing the phase boundary at (λ^*, D^*) .

(c) $D=0.55$, with λ varying between 0.017 and 0.022, crossing the critical line λ_- .

(d) $D=0.3$, with λ varying between 0.0001 and 0.00036, again crossing λ_- .

(See Fig. 1.) Case (a) serves as a check on the method (RFT-type critical behavior along this line was estab-

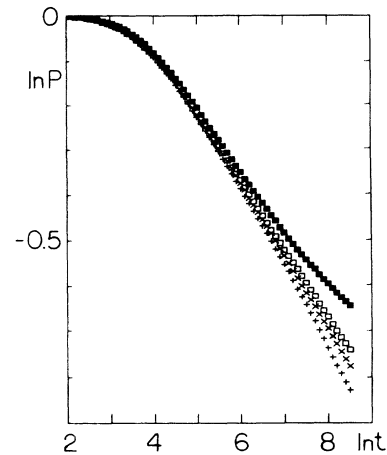


FIG. 2. Survival probability P_t vs time from simulation of the triplet annihilation model with $\lambda=0.1$, and various diffusion rates. +, $D=0.58$; \times , $D=0.585$; \square , $D=0.59$; \blacksquare , $D=0.60$.

lished in Ref. 15), while cases (b)–(d) represent unknown territory. In cases (a) and (b), the maximum duration of a run t_M was 5000; $t_M=10\,000$ in case (c). In case (d) the creation rate is two orders of magnitude smaller than in case (c), and the evolution is commensurately slower. The maximum duration was therefore set at 500 000, and a cluster of three particles was used as the initial configuration. A lattice of 2000 sites sufficed to avoid particles arriving at the boundary in cases (a)–(c); 6000 sites were used in case (d). Between 20 000 and 50 000 runs were executed for each pair (λ, D) of parameter values studied in cases (a)–(c); considerations of computer time limited the sample size to 8000 in case (d).

Typical results are shown in Figs. 2–4, which depict P_t , n_t , and x_t^2 , respectively, for case (b). (The other cases show a similar scaling behavior.) The corresponding local slopes— δ_t , defined in Eq. (5), and η_t and z_t (defined analogously)—are plotted versus t^{-1} in Figs. 5–7. From these plots it is clear that P_t , n_t , and x_t^2 exhibit an asymptotic power-law behavior. The curvature of the P_t and n_t plots for off-critical parameter values is also quite distinct. [In cases (a) and (c) this curvature is less evident, and the critical creation rate λ_c can be estimated from

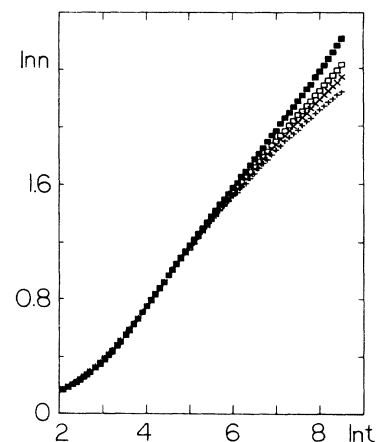


FIG. 3. Mean particle number n_t vs t . Symbols as in Fig. 2.

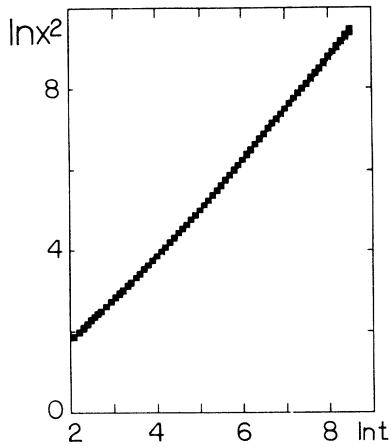


FIG. 4. Mean-square displacement of particles x_t^2 vs t . Symbols as in Fig. 2.

the δ_t and η_t graphs: distinct curvature as $t \rightarrow \infty$ marks an off-critical value.] Once the critical parameters have been bracketed, the critical exponents can be estimated from the asymptotic behavior of the local-slope graphs. The estimates for the location of the phase boundary and the critical exponents are given in Table I. The phase-

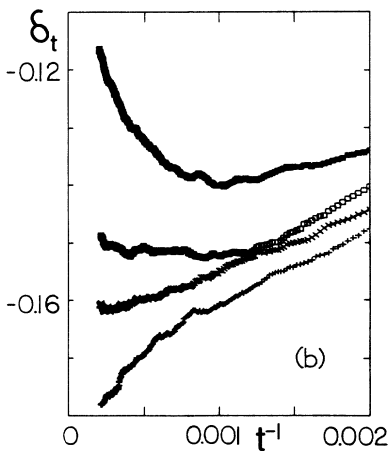
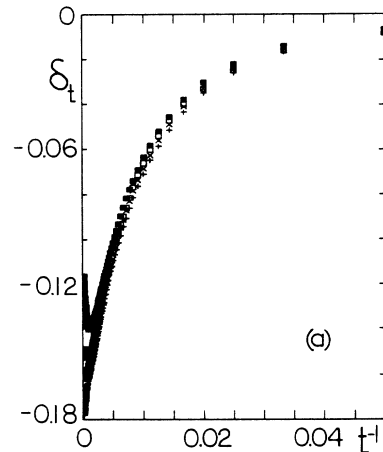


FIG. 5. (a) Local slope δ_t associated with the decay of the survival probability vs t^{-1} . Symbols as in Fig. 2. (b) Long-time behavior of δ_t .

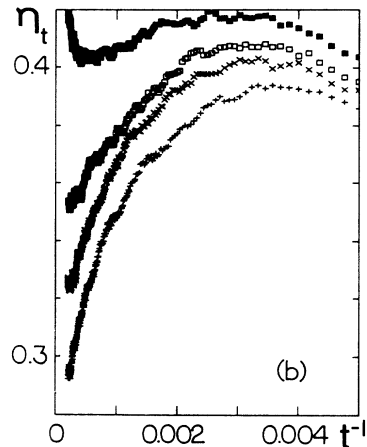
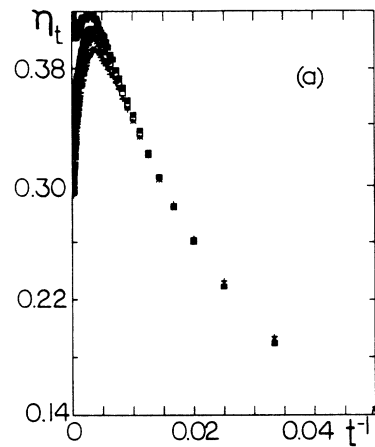


FIG. 6. (a) Local slope η_t associated with the growth in the particle number vs t^{-1} . (b) Long-time behavior of η_t .

boundary estimates are in good agreement with the steady-state simulation results.¹⁵ The critical exponent estimates for cases (a)–(d) are all in agreement with the standard RFT values.

While the ultimate power-law behavior is the same in all cases, interesting differences may be observed in the transient dynamics. Case (a), which represents the “nor-

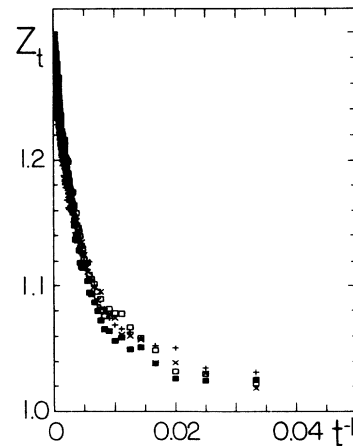


FIG. 7. Local slope z_t associated with the mean-square displacement vs t^{-1} . Symbols as in Fig. 2.

TABLE I. Critical parameters and exponents from time-dependent simulations of the triplet annihilation model. Numbers in parentheses denote the uncertainty in the last figure(s).

Case	λ_c	D_c	δ	η	z
(a)	0.721(2)	0.5	0.156(2)	0.32(1)	1.27(2)
(b)	0.1	0.587(4)	0.160(5)	0.34(3)	1.27(2)
(c)	0.0205(15)	0.55	0.160(5)	0.35(3)	1.28(2)
(d)	0.000 24(5)	0.3	0.154(8)	0.33(2)	1.24(3)
RFT (standard values ^a)			0.162(4)	0.317(2)	1.272(7)

^aFrom Refs. 9 and 11.

mal" situation of extinction due to insufficiently rapid creation, shows a linear trend in the local slopes. This is consistent with a correction-to-scaling exponent $\delta' = 1$, as expected for directed percolation in $d = 1 + 1$.²⁷ Cases (b) and (c), which are diffusion dominated, have linear local-slope plots only at very late times. In these cases the P_t plot is initially flat, reflecting the fact that annihilation is unlikely at early times, since triplets are rare. In the absence of significant annihilation, the initial growth in n_t is exponential, albeit at a slow rate. This is seen in Fig. 3, which also shows a crossing effect: the plot with the largest population n_t at short times has the smallest population at long times. It is also worth noting that the diffusive behavior is generally insensitive to variations in λ and D . Thus plots of x_t^2 and z_t yield the exponent z , but are of no assistance in locating the critical point. In cases (c) and (d), diffusion is essentially normal ($z_t \cong 1$) in the early phase of the dynamics, and then approaches RFT-type behavior somewhat abruptly. The late and nonuniform approach to scaling behavior in cases (c) and (d) presumably reflects a crossover to RFT behavior at late times, following an early stage which is dominated by a different critical behavior associated with $\lambda \rightarrow 0$ and $D \rightarrow 0$. (The latter has not been studied in simulations.) The slow approach to scaling is likely connected with the difficulties encountered (in the steady-state simulations of Ref. 15) in determining the exponent β on the critical line λ_- .

V. DISCUSSION

The central conclusion to be drawn from the simulations is that the triplet annihilation model exhibits

directed-percolation or RFT-type critical behavior at the four representative points investigated. It seems quite reasonable to extend this conclusion to the entire phase boundary of the model. This result once again underscores the high degree of universality in the critical behavior of reaction-diffusion and related models: all transitions to a unique absorbing state have been found to belong to the RFT class.

The present result of uniform behavior along the phase boundary of the triplet annihilation model is the simplest outcome one could expect. Understanding the phase diagram still poses a serious challenge, however. In particular, it is not clear, in a field-theoretic description, how an *increasing* creation rate causes the disappearance of the active state, nor how the diffusion rate, which ordinarily merely sets the scale for a "temperaturelike" variable, can change the phase diagram qualitatively. The bare parameters λ and D somehow form renormalized creation and diffusion rates which govern the evolution over long times and distances, but the details have not been worked out. An important open question is how a field-theoretic description of nonequilibrium processes should reflect local kinetic rules.^{13,25}

ACKNOWLEDGMENTS

I wish to thank Professor Peter Grassberger, Wolfgang Renz, and Geoffrey Grinstein for helpful discussions. The simulations were performed on the facilities of the University Computing Center of the City University of New York.

¹G. Nicolis and I. Prigogine, *Self-organization in Nonequilibrium Systems* (Wiley Interscience, New York, 1977).
²H. Haken, *Synergetics* (Springer-Verlag, New York, 1983).
³R. M. Ziff, E. Gulari, and Y. Barshad, *Phys. Rev. Lett.* **56**, 2553 (1986).
⁴R. Dickman, *Phys. Rev. A* **34**, 4246 (1986).
⁵S. Katz, J. L. Lebowitz, and H. Spohn, *Phys. Rev. B* **28**, 1655 (1983); *J. Stat. Phys.* **34**, 497 (1984).
⁶F. Schlögl, *Z. Phys.* **253**, 147 (1972).
⁷T. E. Harris, *Ann. Probab.* **2**, 969 (1974).
⁸T. M. Liggett, *Interacting Particle Systems* (Springer-Verlag, New York, 1985), Chap. VI.

⁹P. Grassberger and A. de la Torre, *Ann. Phys. (N.Y.)* **122**, 373 (1979).
¹⁰H. K. Janssen, *Z. Phys. B* **42**, 151 (1981).
¹¹R. C. Brower, M. A. Furman, and M. Moshe, *Phys. Lett.* **76B**, 213 (1978).
¹²J. L. Cardy and R. L. Sugar, *J. Phys. A* **13**, L423 (1980).
¹³P. Grassberger, *Z. Phys. B* **47**, 465 (1982).
¹⁴R. Dickman and M. Burschka, *Phys. Lett. A* **127**, 132 (1988).
¹⁵R. Dickman, *Phys. Rev. B* **40**, 7005 (1989).
¹⁶I. Jensen, H. Fogedby, and R. Dickman, *Phys. Rev. A* **41**, 3411 (1990).
¹⁷T. Aukrust, D. A. Browne, and I. Webman, *Europhys. Lett.*

- 10, 249 (1989).
- ¹⁸T. Ohtsuki and T. Keyes, *Phys. Rev. A* **35**, 2697 (1987).
- ¹⁹D. Elderfield and D. D. Vvedensky, *J. Phys. A* **18**, 2591 (1985);
D. Elderfield and M. Wilby, *ibid.* **20**, L77 (1987).
- ²⁰G. Grinstein, Z.-W. Lai, and D. A. Brown, *Phys. Rev. A* **40**,
4820 (1989).
- ²¹R. Dickman, *J. Stat. Phys.* **55**, 997 (1989).
- ²²In Ref. 15 the creation rate is denoted by η . In the present
work η is reserved for its traditional role, denoting one of the
critical exponents.
- ²³M. C. Marques, *Physica A* **163**, 915 (1990).
- ²⁴P. Grassberger, *J. Phys. A* **22**, 3673 (1989).
- ²⁵P. Grassberger, *J. Phys. A* **22**, L1103 (1989).
- ²⁶W. Kinzel, in *Percolation Structures and Processes*, edited by
G. Deutscher, R. Zallen, and J. Adler (Hilger, Bristol, 1983).
- ²⁷J. W. Essam, K. De'Bell, J. Adler, and F. M. Bhatti, *Phys.*
Rev. B **33**, 1982 (1986).